19

Reflective Optical Arrays

S. Lagomarsino, I. Bukreeva, A. Surpi, A.G. Michette, S.J. Pfauntsch, and A.K. Powell

Abstract. In this chapter the prospects of using grazing incidence reflection from custom built nested mirrors or reflector arrays are discussed. The aim is to provide a high gain in focused intensity from either laboratory or synchrotron sources. The calculated performances of such systems are presented, taking into account manufacturing tolerances and surface roughness. These calculations indicate that the improvement of roughness is of primary importance, and ways of addressing this during possible manufacturing processes are discussed.

19.1 Introduction

X-ray reflective mirrors are widely used in both synchrotron radiation and laboratory sources to collimate or focus X-ray beams with high efficiency. Improvements to fabrication technologies now allow manufacture of long X-ray mirrors with slope errors less than 1 μrad and root-mean-square (rms) roughnesses less than 0.1 nm [1–3]. In the Kirkpatrick–Baez geometry, such mirrors can provide significantly sub-micrometre focal spots. However, these systems are very expensive and, in general, only large-scale facilities can afford high precision mirrors. To improve flexibility, adaptive mirrors using benders to give the required shapes have been developed [1] but alignment, stability and optimisation of the curvature are critical issues.

If a given spot size is desired, i.e., if a given demagnification factor at a certain distance from the source is required with high focusing efficiency, the length of the mirror should not exceed an optimum value [4]. The flux density of photons in the focal spot can be increased significantly compared to that from a single surface if a system of confocal mirrors, similar to those used in astronomy, is employed [5].

Mono- and poly-capillaries [6, 7] and microchannel plate arrays [8, 9] have also been used for X-ray optics. These work by grazing incidence reflections along many small diameter channels, up to about 10^6 for poly-capillaries and microchannel plates. They can have large apertures and bandpasses, with

transmission efficiencies of several tens of percent. If there are two reflections from the same wall of each channel, they can approximately satisfy the Abbe sine condition [10], thereby reducing coma. If there are more than two reflections, correspondence between object and image points may be lost. Current manufacturing methods, in which optical fibres undergo several stages of pulling [7, 11], limit channel diameters to $\sim$0.5 µm, arrays to a few millimetres square and focal spots to $\sim$10 µm. Performances are limited by channel tilting, curvature errors, waviness, diffraction, uncontrolled substrate bending and defects, i.e., misplaced channels [12]. In addition, microchannel plates are primarily made for another purpose, i.e., X-ray detection, so that they are not optimised for optical performance; for example, the channel wall roughnesses are not a major concern for X-ray detection. Such optics can also have very poor point spread functions [13]; in principle, it is possible to improve their performances by using specific designs – microstructured optical arrays (MOAs) [14]. These may also allow adaptivity and controllable focal length [15].

In the following sections, the performances of such optics will be presented, along with discussions of fabrication routes to compact systems adaptable to a large range of photon energies and X-ray sources. These systems can be tailored to be focusing, collimating or condensing devices.

19.2 Nested Mirror Systems

Nested mirror systems use arrays of confocal reflecting surfaces such as shown in Fig. 19.1. In this example of elliptical mirrors, rays emanating from one focus F_1, common to all the mirrors, converge after reflection to the second common focus F_2. It is worth noting that, in general, the mirrors do not have to be elliptical; the shape depends on the application.

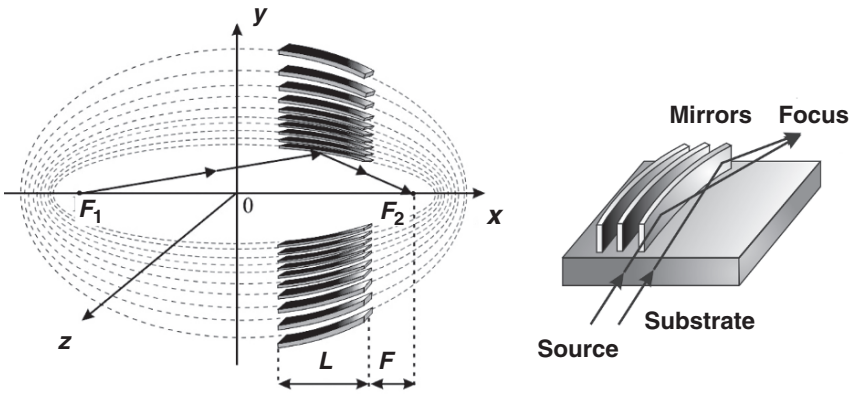

Fig. 19.1. Nest of confocal elliptical mirrors

19.2.1 Computer Simulations

The proper choices of system configuration and material for the reflecting surfaces are very important. For optimisation of the relevant parameters and evaluation of the fabrication tolerances, a computer ray-tracing code allowing parallel treatment of the optical elements has been developed [16, 17]. This code gives information about the intensity distribution in the focal spot, the system efficiency and the gain. Gain is defined as the ratio between the output and input flux densities, and corresponds to the enhancement in intensity with respect to a hypothetical aperture of the same size as the focal spot placed in the focal position. The code has been used to evaluate nested mirror systems for a synchrotron radiation source and for a laboratory-scale source.

For the synchrotron, a bending magnet source of the European Synchrotron Radiation Facility, namely the optical beamline BM5, was used as an example. A geometry which focuses the beam in the horizontal plane was considered, with a horizontal source size of 270 μm, a divergence of 2.4 mrad, a source-focus distance of 40 m and a wavelength of 0.1 nm. The focusing system (Fig. 19.2) has four nickel mirrors with length of 25 mm, height of 300 μm and wall thicknesses of 37 μm at the entrance and 20 μm at the exit. The simulations indicate that this system can focus the incident beam into a spot of ≈0.14 μm full width at half maximum (FWHM) at 1 cm from the exit edge of the system, with a gain of around 980.

For the laboratory-scale microfocus source, a focused electron spot size of 15 μm, a wavelength of 0.154 nm and a source-focus distance of 150 mm were assumed. The optimised system in this case has two symmetrical nickel mirrors of length 25 mm, height 300 μm and wall thickness 100 μm (Fig. 19.3). This provides focusing into a spot of around 0.8 μm FWHM, 5 mm from the exit edge of the system, and a gain of around 90.

A variety of characteristic distortions in technological processing and errors that are inevitably introduced during manufacture can both lower the

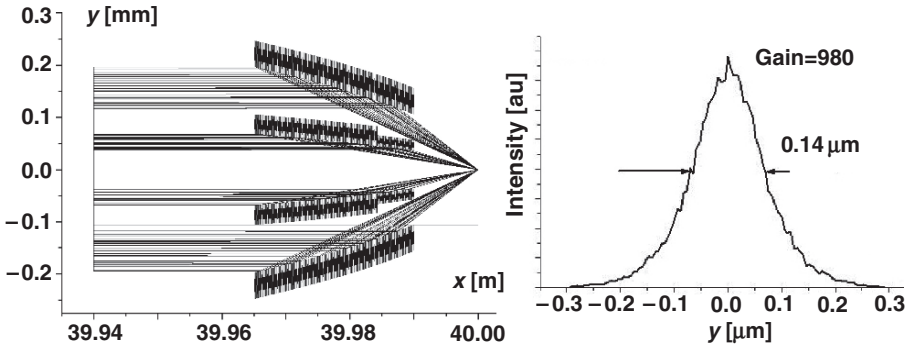

Fig. 19.2. Results of optimisation: (*left*) an optical system for a synchrotron radiation source and (*right*) the distribution of intensity in the focal spot

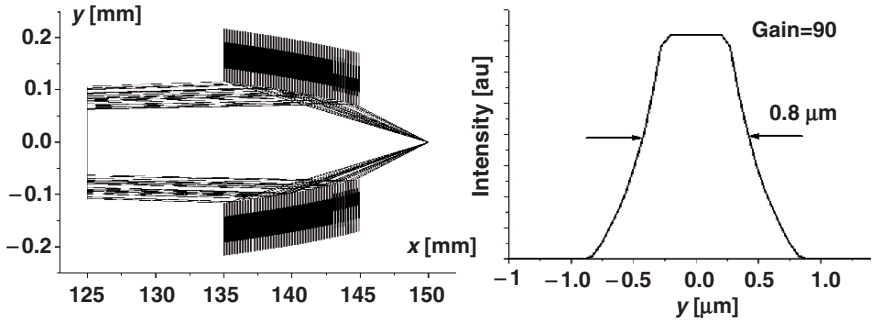

Fig. 19.3. Results of optimisation: (*left*) an optical system for a laboratory-scale microfocus source and (*right*) the distribution of intensity in the focal spot

reflectivity and broaden the focal spot leading to significant reduction in the gain. Simulations have therefore been carried out to take into account various deviations from the ideal design, including slope error, relative shift of the mirrors and poor wall verticality, i.e., the angular inclination of the walls with respect to the axis normal to the surface. To minimise deviations which cause blurring at the scale of the focal spot size, for the synchrotron radiation source, the slope error should be less than 2 μrad, relative shifts of the mirrors should not exceed 0.16 μm and the wall verticality should be better than 1.5 mrad. For the microfocus source, the fabrication tolerances are not so tight but are still quite severe. The slope error must be better than 30 μrad, relative shifts of the mirrors must be smaller than 1 μm and wall verticality must be better than 6 mrad.

The surface roughness required for efficient mirrors can be estimated from the amount of power reflected in the specular direction. Using the simple Debye–Waller model, the total intensity I in the geometrically focused beam is given approximately by

$$I = I_0 \exp\left(-\left(\frac{4\pi\sigma \sin\theta}{\lambda}\right)^2\right), \tag{19.1}$$

where I_0 is the intensity in the absence of roughness, σ is the rms surface roughness and θ is the grazing incidence angle. To obtain 50% power into the geometrical image and with $\theta \sim 3$ mrad, the surface roughness must satisfy $\sigma < 2$ nm for photon energies around 12 keV.

19.2.2 Mirror Fabrication Procedures

As discussed in Sect. 19.2.1, the tolerance limits are rather tight, especially for synchrotron radiation sources. Thus, control of the fabrication process is critical and advanced procedures are required. Moreover, in addition to the accuracy requirements in shape and positioning, etc., it is important to have

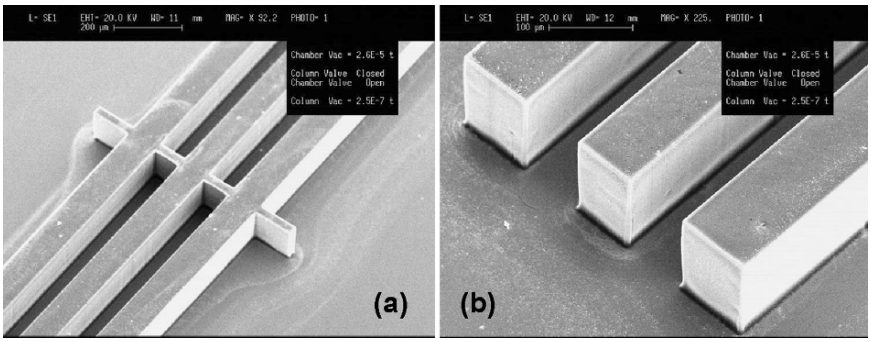

Fig. 19.4. (**a**) A mirror system in SU8 resist fabricated using process steps involving electron-beam and optical lithography. A bridge aimed at mechanically reinforcing the structure is visible. (**b**) A detailed view of the system shown in (**a**)

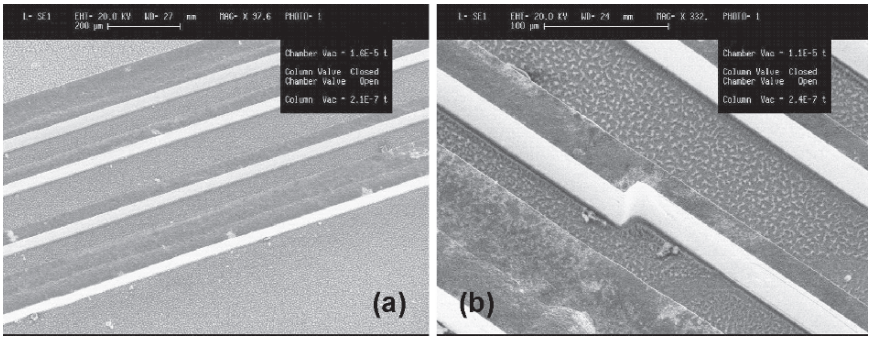

Fig. 19.5. (**a**) A nickel mirror system made using electron-beam and deep X-ray lithography and electro-deposition. (**b**) An enlarged view of the mirror system shown in (**a**)

long structures in the direction of the optical axis, at least in the hundreds of micrometres range, to allow significant acceptance of radiation, as suggested by Fig. 19.1. Thus, if the system is composed of more than two symmetrical mirrors as, e.g., in Fig. 19.2, the aspect ratio must be high, typically greater than 10. If only two mirrors are used, as in the case of the system for laboratory sources shown in Fig. 19.3, large structures and low or moderate aspect ratios are sufficient.

To satisfy these requirements, several fabrication routes can be followed, involving one or more of electron-beam lithography (always necessary to define the shape of the reflecting surface with sufficient precision), optical lithography, X-ray lithography and electro-galvanic growth of material [17]. Figure 19.4 shows a prototype made directly in SU8 photoresist by optical lithography using a mask made by electron-beam lithography. A second prototype is shown in Fig. 19.5; this was made in electro-deposited nickel after electron-beam and X-ray lithography steps.

In both cases, the mirrors follow the design shape, and the overall structures are satisfactory. The main problem is the wall roughness which presently exceeds the acceptable limits. Very recent results on post-fabrication treatment have given interesting indications of possible routes to reduce wall roughness significantly. This will be discussed in Sect. 19.3.2.

Despite the technological problems related to fabrication issues, such systems are very promising, with the great advantages of flexibility and compactness. Using modern microfabrication tools, mirrors of virtually any shape can be manufactured, so that focusing, collimating or condenser systems can be easily designed for different types of source.

Here, simulations involving just one reflection have been presented, but systems working with more reflections (see also Sect. 19.3), including whispering galleries [18], can be conceived. Since an entire system has lateral dimensions of the order of 0.5 mm, several systems with different characteristics can be arranged side by side, allowing easily interchangeable optics. Another aspect of flexibility is provided by the wide operating energy range of such reflective optics.

19.3 Microstructured Optical Arrays

MOAs [14,15], as shown schematically in Fig. 19.6, work on the same principles as poly-capillary and microchannel plate optics. Now, however, the reflecting channels are made to specific designs and are, for example, etched into thin silicon (100–200 μm) which can be flexed to provide adaptivity and/or focal length control. To reduce aberrations such as coma, two reflections are needed in such systems; since the channel lengths are small (due to the thin silicon), reflections from two successive components must be used. In Fig. 19.6, the channel widths are shown as increasing radially outwards, to compensate for the increased grazing incidence angle. In practice, to date, this has not been necessary as achievable aspect ratios (i.e., the ratio of channel length to channel width), means that most X-rays pass straight through without reflecting,

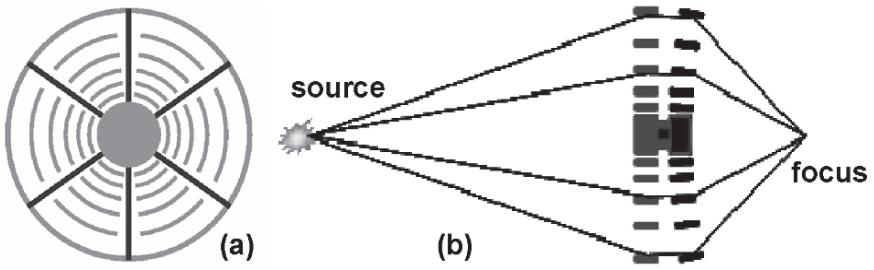

Fig. 19.6. (**a**) A microstructured optical array, face on, and (**b**) arrangement of two MOAs, in which either or both can be flexed to change the position of focus

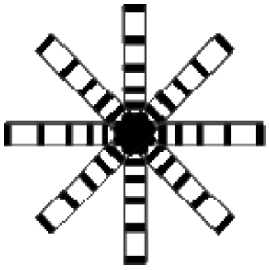

Fig. 19.7. An MOA consisting of an arrangement of 1D strips to give a 2D focus

whatever the radial distance. Additionally, in practice, many more channels would be used compared to the number shown in the schematic diagram; typically channels would be $\sim$10 µm wide, with walls of comparable thickness, over areas of a few square millimetres.

Flexing may be carried out either mechanically or by coating piezo material on, for example, the spokes shown in Fig. 19.6a. By controlling each piece of piezo independently, the X-ray beam could be further manipulated, for example to reduce aberrations in an adaptive or active way.

The two-dimensional focusing capabilities of such arrays could be simulated by making a series of 1D strips, as shown schematically in Fig. 19.7. As well as being technically less challenging to manufacture each strip could also be flexed independently. Other arrangements, designed for specific applications, would also be possible.

19.3.1 Computer Simulations

Modelling the performances of MOAs, even in the simplest way, is challenging. It requires both finite element analysis (FEA), to determine the effect of flexing on the channel walls, and ray tracing to characterise the optical performances. More sophisticated analyses will require wavefront propagation and studies of the effects of diffraction.

FEA and ray tracing are both complicated for such optics, as the effects of many channels have to be taken into account. For FEA, this means that the number of elements to be analysed is very large, leading to problems with mesh sizes, while ray tracing has to be carried out non-sequentially as at most two optical surfaces out of many hundreds will be encountered by an individual array. So far, only rudimentary FEA studies have been carried out, but many characteristics of the optical performances have been investigated using the optical design software ZEMAX©. Recently, ray-tracing analysis has been carried out using the much more flexible (and user-friendly) "Q" software developed at the University of Leicester (UK) [19].

As an example, a silicon MOA designed for X-rays of energy 4.5 keV (Ti K_α) has been modelled using ZEMAX©. This type of optic will be suitable for irradiating cells, in studies related to cancer research, using an X-ray

Table 19.1. Parameters of the prototype MOA for the Gray Cancer Institute microprobe

Source size	5 µm
Source to optic distance	160 mm
Diameter of optic	2 mm
Separation of optic components	1 mm
Length of channels	200 µm
Width of channels	10 µm
Bending radius of first component	∞
Bending radius of second component	100 mm
Focal distance	73 mm

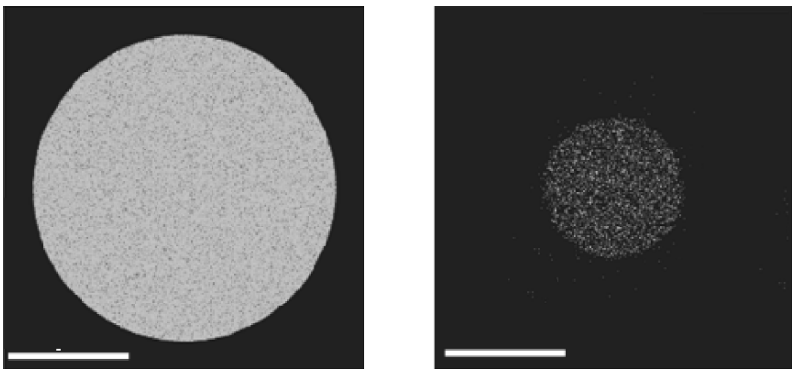

Fig. 19.8. Results of ray tracing the MOA for the Gray Cancer Institute microprobe. The source (*left*) emitted 4.5×10^6 keV photons, of which (*right*) 8,600 were doubly reflected and brought to focus. The scale bars are 2 µm

microprobe at the Gray Cancer Institute (UK) [20]. The parameters are shown in Table 19.1.

The bending radius of the second component (the first was unbent) was chosen to give a focal spot size of about 2 µm, assuming a 5 µm diameter source. Although zone plates can give smaller focal spots than this, the intention was, in the first instance, to aim for something experimentally feasible at an early stage, while providing a focal spot size useful for studies using the microprobe. Smaller spot sizes could be achieved by using a smaller bending radius, or by bending both components. Although this would mean that fewer X-rays would pass straight through without reflection, the effects of roughness would be more pronounced and a detailed analysis needs to be carried out to determine the optimum configuration.

The ray tracing took into account the efficiency of each reflection, which decreases radially outwards as the grazing incidence angle increases, as well as the channel wall roughness. Results for zero roughness (Fig. 19.8) indicate that the configuration of Table 19.1 results in a focusing efficiency of slightly

under 1% (primarily since most X-rays pass straight through). However, the focused flux is some two orders of magnitude higher than that which could be achieved by a state-of-the-art zone plate with a diameter ∼100 μm. A channel wall roughness of 10 nm, the effects of which were modelled using (19.1), reduces this gain by a factor of about 3, suggesting that a roughness of a few nanometres is acceptable at energies of a few keV. An additional advantage of MOAs, over zone plates, is that the focal length is independent of energy, so that (unless energy-dependent effects are being studied) the bremsstrahlung as well as the characteristic radiation could be used, enhancing the gain in useful flux. To date, using zone plates, all studies using the microprobe have been concerned with cell death [21], rather than the much more important phenomenon of mutation which occurs at a rate several orders of magnitude lower; hence the need for increased focused flux.

19.3.2 Manufacture of Microstructured Optical Arrays

Because of the necessity for high aspect ratios, techniques such as the Bosch process [22] of deep etching in silicon are required to manufacture MOAs. The Bosch process utilises successive etch/passivate stages to create the channels while preventing side-wall etching. Until recently, the applications of such manufacture did not require tight tolerances on wall roughness, and so values of the order of micrometres were acceptable. MOAs require improvements of around three orders of magnitude over this, and so new procedures have had to be devised. By shortening the etch/passivate cycle time, the Scottish Microelectronics Centre at the University of Edinburgh has shown that channel wall roughnesses of less than 20 nm are possible. Subsequent coating with 100 nm of silicon dioxide improved this further to less than about 10 nm [23], which suggests that the ultimate goal of roughnesses of a few nanometres is achievable.

19.4 Conclusions

The nested and array systems presented here show promising capabilities as future generation X-ray optics. Some technological challenges, including roughness, appear close to being overcome, while others, e.g., control of surface shapes for adaptive systems, must still be addressed in detail.

Recent experiments involving coating of nested mirror systems with silica sol-gel showed very promising wall roughness reduction, and 50% reflectivity at Cu line from SU8 walls coated with sol-gel.

Acknowledgments

In addition to the European Science Foundation support, the work on Microstructured Optical Arrays is part of that being carried out by the UK Smart X-Ray Optics (SXO) consortium funded by the Basic Technology Programme

of Research Councils UK (grant code EP/D04880X/1). The members of the SXO consortium are University College London (including the Mullard Space Science Laboratory), King's College London, the Gray Cancer Institute, the Scottish Microelectronics Centre at the University of Edinburgh, the University of Birmingham, the University of Leicester and STFC Daresbury Laboratory. Silson Ltd is an associate member. IFN acknowledges partial financial support from National project SPARX.

References

1. O. Hignette, G. Rostaing, P. Cloetens, A. Rommeveaux, V. Ludwig, A. Freund, Proc. SPIE **4499**, 105 (2001)
2. K. Yamamura, K. Yamauchi, H. Mimura, Y. Sano, A. Saito, K. Endo, A. Souvorov, M. Yabashi, K. Tamasaku, T. Ishikawa, Y. Mori, Rev. Sci. Instrum. **74**, 4549 (2003)
3. Y. Mori, K. Yamauchi, K. Yamamura, H. Mimura, Y. Sano, A. Saito, K. Ueno, K. Endo, A. Souvorov, M. Yabashi, K. Tamasaku, T. Ishikawa, Proc. SPIE **4782**, 58 (2002)
4. I.N. Bukreeva, S.B. Dabagov, S. Lagomarsino, Appl. Opt. **43**, 6270 (2004)
5. C.G. Cheng, R.K. Heilmann, P.T. Konkola, O. Mongrard, G.P. Monnely, M.L. Schattenburg, J. Vac. Sci. Technol. B **18**, 3272 (2000)
6. H.N. Chapman, K.A. Nugent, S.W. Wilkins, Rev. Sci. Instrum. **62**, 1542 (1991)
7. M.A. Kumakhov, Proc. SPIE **3444**, 424 (1998)
8. S.W. Wilkins, A.W. Stevenson, K.A. Nugent, H. Chapman, S. Steenstrup, Rev. Sci. Instrum. **60**, 1026 (1989)
9. G.W. Fraser, J.E. Lees, J.F. Pearson, M.R. Sims, K. Roxburgh, Proc. SPIE **1546**, 41 (1992)
10. J.F. McGee, A Catoptric X-Ray Optical System (for Use in Laser-Fusion Diagnostics). Final Technical Report, Saint Louis University, Missouri, 1982
11. J.L. Wiza, Nucl. Instrum. Methods **162**, 587 (1979)
12. M.V. Gubarev, C.D. Bankston, M.K. Joy, J.J. Kolodziejczak, C.E. McDonald, C.H. Russell, W.M. Gibson, Proc. SPIE **3444**, 467 (1998)
13. A.N. Brunton, G.W. Fraser, J.E. Lees, I.C.E. Turcu, Appl. Opt. **36**, 5461 (1997)
14. P.D. Prewett, A.G. Michette, Proc. SPIE **4145**, 180 (2000)
15. A.G. Michette, P.D. Prewett, A.K. Powell, S.J. Pfauntsch, K.D. Atkinson, B. Boonliang, J. Phys. IV France **104**, 277 (2003)
16. I. Bukreeva, A. Gerardino, A. Surpi, A. Cedola, S. Dabagov, S. Lagomarsino, Proc. SPIE **5974**, 59741D (2005)
17. I. Bukreeva, A. Surpi, A. Gerardino, S. Lagomarsino, F. Perennes, M. Altissimo, S. Cabrini, A. Carpentiero, A. Vicenzo, P. Cavallotti, Opt. Commun. **259**, 366 (2006)
18. V.I. Ostashev, V.E. Asadchikov, I.N. Bukreeva, O.N. Gilev, N.A. Havronin, I.V. Kozhevnikov, S.I. Sagitov, Opt. Commun. **155**, 17 (1998)
19. R. Willingale, http://www.star.le.ac.uk/∼rw/(last accessed 25 April 2007)

20. K.D. Atkinson, M. Folkard, B. Vojnovic, G. Schettino, K.M. Prise, B.D. Michael, A.G. Michette, Radiat. Res. **161**, 103 (2004)
21. M. Folkard, K.M. Prise, C. Shao, S. Gilchrist, A.G. Michette, B. Vojnovic, Acta Phys. Pol. A **109**, 257 (2006)
22. A.A. Ayón, X. Zhang, R. Khanna, Sens. Actuators A **91**, 381 (2001)
23. W. Parkes, Private communication (2006)